10-2-2018

Influence of phosphate on tungstate sorption on hematite: A macroscopic and spectroscopic evaluation of the mechanism

Bryan Sallman
Tennessee State University

Sudipta Rakshit
Tennessee State University

Grégory Lefèvre
Institut de Recherche de Chimie Paris

Recommended Citation

B. Sallman, S. Rakshit, G. Lefèvre, "Influence of phosphate on tungstate sorption on hematite: A macroscopic and spectroscopic evaluation of the mechanism", Chemosphere, Volume 213, 2018, Pages 596-601, ISSN 0045-6535, https://doi.org/10.1016/j.chemosphere.2018.09.157.

Influence of Phosphate on Tungstate sorption on Hematite: A Macroscopic and Spectroscopic evaluation of the Mechanism

Bryan Sallman[a], Sudipta Rakshit[a*], and Grégory Lefèvre[b]

[a]Department of Agricultural and Environmental Sciences, Tennessee State University,

3500 John A. Merritt Blvd., Nashville, Tennessee 37209-1561

[b]Institut de Recherche de Chimie Paris, CNRS-Chimie ParisTech, 11 rue Pierre et Marie Curie,

75005 Paris, France.

[*]Corresponding author. Tel.: +1 615-963-6058; Fax: +1 615-963-5436. E-mail address:

srakshit@tnstate.edu

Abstract

The environmental fate of the tungstate (VI) oxyanion [e.g. mono tungstate and several polytungstate, generally expressed by W (VI)] is largely controlled by sorption on soil minerals, especially on iron oxide minerals. Molecular scale evaluation of W (VI) retention on iron oxides in the presence of competing oxyanions is scarce in literature. Here we report surface interaction mechanisms of W (VI) on hematite in the presence of phosphate (P) using macroscopic and *in situ* attenuated total reflectance Fourier transform infrared (ATR-FTIR) spectroscopic experiments. Batch sorption experiments were conducted using 2g L^{-1} hematite and 100 µM W (VI) and P, in single ion system and in binary mixtures as a function of pH (4-11). *In situ* ATR-FTIR spectroscopic evaluation of P and W (VI) sorption on hematite was also carried out. The results from macroscopic experiments indicated that W (VI) sorption on hematite was not affected by P when W (VI) was added first. The influence of P on W (VI) sorption was noticed when W (VI) & P were added simultaneously or P was added first. The *in situ* ATR-FTIR spectroscopic data corroborated these findings. In addition, the spectroscopic data revealed that in the presence of P, the surface complexation mode of W (VI) differed as noted from either the absence of W-O antisymmetric infrared (IR) band or the W-O-W stretching band. This study provides useful information on molecular level understanding of W (VI) surface complexation on hematite in the presence of competing ions such as P.

1. Introduction

The link between elevated tungstate (W (VI)) concentrations in the tap water, ground water, and tree ring samples to a childhood leukemia cluster in NV highlighted the importance of considering tungsten (W) as an 'emerging contaminant' (EPA, 2017). Even though no conclusive results could be obtained by an investigation led by The Center for Disease Control (CDC) to strengthen this link, the circumstantial evidence encouraged many researchers to perform a thorough investigation on W (VI) toxicity (Sheppard et al., 2006; Steinberg et al., 2007). Experiments on mice suggested that 16 weeks of chronic W (VI) exposure (conc. 15-200 mg L^{-1}) can cause DNA damage and promote tumor development (Kelly et al., 2013). Strigul (2005) found that soil incubated with W powder for 3 months led to the death of 95% of the soil bacteria.

Tungsten (W) is heavily used for domestic and industrial purposes (Koutsospyros et al., 2006). Approx. 86,400 metric tons of W were mined worldwide in 2016 (USGS, 2017) for applications such as tungsten-cemented carbide, military and hunting ammunition, medical equipment, and light bulb filaments (Koutsospyros et al., 2006; Ogundipe et al., 2009). Due to lead (Pb) toxicity, W had replaced Pb in many small caliber military and hunting ammunition rounds by the late 1990s (Fisher et al., 2006; Thomas et al., 2009). In addition to industrial and domestic uses, dissolution of W-bearing minerals was found to be another major source for W (VI) occurrence in the environment (Seiler et al., 2005).

The high provenance of W and its compounds in the environment, as well as suspected toxicity to human and ecological health, prompted many fate studies (Koutsospyros et al., 2006). Soil minerals can control the fate of W(VI) by sorption, and consequently, many studies have

evaluated the sorption mechanisms of W (VI) on various soil minerals (Gustafsson, 2003; Xu et al., 2006, 2009; Lorenz, 2009; Lorenz et al., 2011; Kashiwabara et al., 2013; Davantes and Lefevre, 2015; Sun and Bostick, 2015; Hur and Reeder, 2016; Rakshit et al., 2017). In general, W (VI) displays a high affinity for iron-and aluminum hydr (oxide) minerals (Gustafsson, 2003; Xu et al., 2009; Hur and Reeder, 2016). To support the findings in macroscopic sorption isotherm and envelope, researchers determined molecular level information on the surface retention mechanism using EXAFS and *in situ* ATR-FTIR spectroscopic tools. (Davantes and Lefevre, 2015; Hur and Reeder, 2016; Davantes et al., 2017; Rakshit et al., 2017). These spectroscopic measurements are very sensitive and resulted in detailed information about surface complexes at an environmental W (VI) conc. range (Hur and Reeder, 2016; Davantes et al., 2017; Rakshit et al., 2017).

A challenge of studying the molecular mechanism of W (VI) interaction with mineral surfaces is that the currently available W (VI) solution speciation cannot always be linked to the probable surface complexation at a given solution property. This is because thermodynamic data were unavailable in an environmental W (VI) conc. range (Rakshit et al., 2017). For example, the seminal papers which determined W solution speciation listed conc. range of W (VI) as 0.5-123 mM (Cruywagen and van der Merwe, 1987), 0.5 M (Shijun et al., 1998), 3 M (Smith and Patrick, 2000), and 2 mM (Hur and Reeder, 2016). Interestingly, W (VI) is known to polymerize at higher concentration even at unfavorable pH values (Hur and Reeder, 2016). Thus, extrapolating the solution speciation conducted at mM and M levels to μM should be interpreted carefully.

Although important molecular level information about W (VI)-Fe/Al(hydr)oxide surface complexes at an environmental conc. range is currently available in literature, no studies to the

best of the authors' knowledge determined the nature of surface complexes in the presence of a competing anion such as phosphate (P) using surface sensitive spectroscopic probes. The likelihood of the coexistence of P and W (VI) in the environment is high. Thus, some macroscopic competitive sorption studies with W (VI) and P on Fe/Al(hydr)oxide clay minerals are already available in literature (Gustafsson, 2003; Xu et al., 2009; Iwai and Hashimoto, 2017). These studies indicated that P has influence in reducing W (VI) sorption on Fe/Al-(hydr)oxide minerals. However, due to the lack of molecular level information about probable surface complexes of W (VI) in the presence of P, the fit of surface complexation model (SCM) in the competitive system was not successful in some cases (Gustafsson, 2003). Thus, molecular level spectroscopic studies on P and W (VI) competitive sorption on common iron oxides, such as hematite, are unavailable in literature. Hence, the main objective of this study is to probe the surface interaction mechanism of W (VI) on hematite in the presence of P using macroscopic and *in situ* ATR-FTIR spectroscopic investigations under various solution properties.

2. Materials & Methods

2.1 Reagent and materials

Hematite was synthesized following a procedure described in our earlier study (Rakshit et al. 2017), which was mainly derived from the hematite synthesis procedures published by Sugimoto et al. (1993) and Elzinga and Kretzchmar (2013). In short, 500 mL of 2 M $FeCl_3$ solution was mixed dropwise to a continuously stirred 500 mL 5.4 M NaOH solution within a period of 5 min. The gel-like precipitate was collected in a pyrex glass bottle, sealed, and heated in a drying oven at 101^0C for 8 days. The solid was then cooled to room temperature, washed with Milli-Q water (18.2 MΩ cm) until the EC value was < 5 µS cm^{-1}. The suspension was then

freeze-dried and stored in a dry place at room temperature. The mineral identity was confirmed using X-ray diffraction (Rigaku, Woodlands, TX). The surface area of hematite produced by this procedure is in the range of 24 m^2 g^{-1} (Elzinga and Kretzchmar 2013). Sodium dihydrogen phosphate (NaH_2PO_4) and sodium tungstate (Na_2WO_4, $2H_2O$) were purchased from Sigma Aldrich (St. Louis, MO). This hematite preparation method may be subjected to minor silica contamination.

2.2 Macroscopic Sorption Experiments

Three types of macroscopic batch sorption experiments were conducted to determine the competitive effect of P on W (VI) surface interaction on hematite. These experiments are termed 'W 1^{st}, P 2^{nd}'; 'W, P simultaneous'; and 'P 1^{st}, W 2^{nd}' experiments. These batch sorption experiments were performed in triplicate in 10 mL volumes in an anaerobic chamber (Coy Laboratory Products, Grass Lake, MI) to avoid interference from carbonate during pH control (Leuz et al., 2006). For 'W 1^{st}, P 2^{nd}'', W (VI) stock was added to the hematite suspension (2g L^{-1}) to make 100µM concentration at I =0.01 M NaCl, and at a pH range of 4-11. The suspension was then equilibrated for 24h at a fixed temperature (298K). The pH was controlled using small additions of 0.1 M NaOH and HCl and the final pH value was recorded. The suspension was then centrifuged and decanted carefully to keep the solid in the centrifuge tube. The filtrate was collected to analyze the W (VI) in ICP-OES (iCAP 7400, Thermo Electron, West Palm Beach, FL). The remaining solid was washed with electrolyte solution (i.e. 0.01 M NaCl), centrifuged, and decanted to remove the interstitial sorbate. This wash solution was analyzed by ICP-OES to ensure that the sorbed fraction was not removed. 10 mL of a 100µM P solution was then added to each solid at respective pH values and equilibrated for 24h at 298 K. The filtrate was then collected for analysis in ICP-OES for total W (VI) and P. Appropriate

standards and quality control samples were run in ICP-OES to satisfy the standard quality control/quality assurance protocol.

For 'W, P simultaneous' experiments, 100µM of both W (VI) and P were added simultaneously (10 mL total volume), equilibrated for 24h at 298 K, I = 0.01 M NaCl, and with a pH range of 4-11. The suspension was then centrifuged, decanted, and the filtrate was analyzed for total W and P by ICP-OES. For 'P 1st, W 2nd' experiments, the hematite suspension was equilibrated with 100µM P at pH range of 4-11. After 24h of equilibration at 298K, the content was centrifuged, decanted carefully to save the solid, and filtered. The filtrate was collected to analyze total P by ICP-OES. The solid was washed with 0.01 M NaCl solution to remove any interstitial P in the reaction mixture. The wash solution was collected and measured in ICP-OES to verify if any P was removed from the sorbed phase. 10 mL of W (VI) stock solution was then added in the suspension of P sorbed hematite to attain an initial W (VI) concentration of 100 µM at ionic strength of 0.01 M NaCl, and a pH range of 4-11, equilibrated at 298K for 24h, centrifuged, decanted, and filtered. The filtrate was analyzed for total W and P in ICP-OES. These three types of competitive sorption experiments portray a comprehensive view of the influence of P on sorption of W (VI) on hematite. All wet chemical experiments were performed in triplicates with a mean value and standard deviation plotted. Control experiments without the hematite in the reaction mixture were performed under the same conditions as the treatments above. Negligible change in W (VI) concentrations was noticed. Samples were not stored more than 48h before analyses in ICP-OES.

2.3 Spectroscopic Experiments

Evaluation of molecular level competitive reactions between W and P via *in situ* ATR-FTIR experiments were performed with a Perkin Elmer Frontier Infrared spectrometer equipped

with a liquid N_2-cooled mercury cadmium telluride (MCT-A) detector, a Balston-Parker air purger provided the optics compartment with H_2O- and CO_2-free air. The HATR flow cell was prepared by evenly coating a 45^{o} ZnSe ATR cell (Pike Technologies, Madison, WI) with a hematite suspension (approx. 2.5mg in 500µL suspension) and allowing it to dry overnight. The flow cell was sealed with a top plate, placed on the ATR sample platform of the IR spectrometer, connected to an Ar-purged reaction vessel containing 500 mL background electrolyte solution (0.01M NaCl) with pH maintained at an appropriate value using small volumes of 0.1M NaOH or HCl solution. A peristaltic pump (Watson Marlow 400, Falmouth, UK) circulated the solution from the reaction vessel to the flow cell at a rate of 2 mL min^{-1}. A magnetic stir bar at the bottom of the reaction vessel maintained constant mixing of the solution. This type of flow-cell set up has been used widely in literature and in our previous studies (Elzinga and Sparks, 2007; Rakshit et al., 2013 a, b; Rakshit et al., 2017).

Each experiment began with a preliminary equilibration step, in which the background electrolyte solution was circulated through the HATR flow cell for approx. two hours and several background spectra were collected. After this pre-equilibration time, a final background spectrum was collected at an appropriate experimental pH. All other spectra were collected against a ratio of the final background spectrum so that only IR peaks resulting from the surface interactions between hematite and W (VI) or P were recorded. System pH was maintained at a specific value throughout the experiment. Competitive sorption experiments between W (VI) and P were initiated by introducing one analyte (either W or P) into the reaction vessel and monitoring interactions with hematite substrate via IR absorbance scans in the 1400- 700 cm^{-1} range (Davantes and Le'fevre, 2015, 2017; Rakshit et al., 2017). Sorption was estimated to have reached equilibrium when no further increase in IR band intensity was observed. The final

spectrum was collected, and the process was repeated by maintaining the initial sorbate in the vessel and incorporating the competing sorbate (P or W) in two 100µM concentration intervals. A ratio greater than 1:1 was used to understand the effect of excess concentration of one sorbate on the other. Background corrected raw spectra and difference spectra were presented.

To test the effects of pH in the competitive sorption, a separate *in situ* ATR-FTIR experiment was conducted using 100 µM concentrations of both W (VI) and P. The experiment was initiated at a pH value of 8.01 and both W (VI) and P were introduced through injecting fresh stock solution in the reaction vessel simultaneously to a concentration of 100 µM each. When sorption had reached equilibrium, the final spectrum was recorded and the pH was lowered to the next level. These steps were repeated until a pH value of 4.6. Since W (VI) is known to polymerize at acidic pH values, the reaction was initiated at alkaline pH values.

2.4 Polyoxometalate Formation

The possibility of the formation of tungstophosphoric acid in the solution has been tested indirectly using *in situ* ATR-FTIR spectroscopy. Since we removed supernatant solute concentrations for P first and W first experiments before adding either W or P in the reaction mixture, the formation of polyoxometalate or more specifically, tungstophosphoric acid (TPA), was not expected in those experiments. There was a possibility of polyoxometalate formation when binary mixtures of P and W (VI) were added simultaneously to the hematite suspension in the batch sorption experiments. *In situ* ATR-FTIR time series data of TPA was compared with that of simultaneous, P first and W first adsorption systems (Fig. S2 A, B) having similar solution properties. The IR bands responsible for P binding on hematite were significantly different in TPA compared to the P and W (VI) binary systems. In TPA, there is a greater amount of W (VI) than P (12:1), which is evident by the IR band intensities that resulted from

the sorption of TPA on hematite (i.e. greater intensity for the 932 cm^{-1} band than the 1082 cm^{-1} band). For the sorption experiments with P & W (VI) binary mixtures (1:1 and 2:1), different features were observed, i.e., intensity of the IR bands for P was always greater than W. In TPA the amount of W (VI) is always greater than P. Thus, we did not find any evidence of TPA formation in our experimental systems.

3. Results & Discussion

3.1 Effect of pH

a) Single Ion System: The tungstate (W (VI)) sorption envelope on hematite indicated approx. 100% sorption until pH 7.7 and a gradual decrease of sorption to approx. 50% at pH 10 (Figure 1A). The sorption envelope indicated negligible ionic strength dependence until pH 7.7. After this point, increasing ionic strength led to increased sorption. Both the lack of ionic strength dependence and increasing sorption with increasing ionic strength when sorption is less than 100% (i.e. pH>7) suggests an inner-sphere mode of surface interactions (Hayes et al., 1988; McBride, 1997). For W (VI) sorption on goethite, Xu et al. (2006) reported 100% sorption until pH 5. Sorption decreased by 50% at pH 7 and by 80% at pH 10. Thus, the sorption envelope indicated a much sharper decrease in W sorption on goethite. Interestingly, for W (VI) sorption on ferrihydrite (containing 1 mM Fe), Gustafsson, (2003) reported that approximately 100% of W (VI) sorbed until pH 7.5. After that point, sorption gradually decreased to a value of 40% at pH ~9.2. Detailed mechanistic interpretations of the effects of pH on W (VI) sorption on hematite were published in our earlier study, in which *in situ* ATR-FTIR spectroscopy was used to probe the surface interaction mechanisms (Rakshit et al., 2017). The authors noted that at

lower pH values, the IR bands intensified due to the formation of inner-sphere type bonding. A gradual shift of the W-O stretching band to a higher wavenumber upon decrease of pH value corroborated this mechanistic finding as well.

b) Binary Mixtures with Phosphate: Three different systems were evaluated, in which W (VI) was added first (W 1st, P 2nd), P was added first (P 1st, W 2nd), and W (VI) and P were added simultaneously (Fig. 1B). These three sorption envelopes were plotted along with W (VI) single ion system at 0.01 M ionic strength to compare sorption in the presence and absence of P. When W (VI) was added first, addition of P at a1:1 ratio did not show any effect on the sorption envelope. Only a minor reduction of sorption (2-4%) compared to W (VI) alone system was noticed at pH 10. Major differences in sorption were noted when W (VI) and P were added simultaneously or when P was added first. In both cases, the sorption envelope indicated that retained W (VI) was reduced by approx. 30% as pH was raised above a value of 7. A similar difference was noticed at pH 4 for the 'P 1st, W 2nd' system.

Gustafsson, (2003) reported no competitive effect of 200 µM P on 50 µM W (VI) sorption on ferrihydrite at lower pH until a pH value of 5.5. W (VI) sorption on ferrihydrite decreased by approx. 25% and 60% at pH 6.5 and 7.5, respectively, in the presence of P. For the hematite used in our study, the sorption reduction at these pH values was lower (~ 30% at pH 7). The diminished effects of P in our study could be due to the lower amount of P (i.e. 100 µM) used in the competitive sorption experiments compared to that of Gustafsson (200µM), (2003). The chosen P concentration in our case was to mimic a practical environmental concentration range (Goldberg, 2010). Detailed interpretations of the mechanisms underlying these macroscopic competitive sorption experiments were noted in the next section, in which *in situ* ATR-FTIR analyses of competitive sorption of P and W (VI) in binary mixtures were reported.

3.2 Analysis of *in situ* ATR-FTIR Spectra of W (VI) and P Binding on Hematite

a) Time Series Spectra: *In situ* ATR-FTIR spectra of competitive sorption of W (VI) and P on hematite were presented in Figures 2 A & B. The corresponding difference spectra were noted in Figures 2 A1 & B1. In Figure 2A, the time series spectra indicated the competitive sorption system of W (VI) and P, in which W (VI) was added first and equilibrated before P addition. For clarity, only final equilibrated W (VI) spectrum was shown in Figure 2A. This spectrum illustrated IR bands associated with W-O symmetric (930 cm^{-1}) and antisymmetric (830 cm^{-1}) stretching due to strong inner-sphere type surface complexation of W (VI) with the hematite surface as reported by earlier studies (Zorina and Syritso, 1972; Charton et al., 2002; Tomaszewicz et al., 2009; Kumar and Mohanta, 2011; Tribalis et al., 2014; Davantes and Lefevre, 2015; Rakshit et al., 2017). Subsequent time series spectra after 100 µM and 200 µM P additions were depicted to indicate the gradual growth of 1082 cm^{-1} IR band due to P surface complexation on hematite in the W +P mixed system (Figure 2A). The spectral subtraction of the W (VI) only system from the mixed system resulted in the difference spectra (2A1), which indicated that the addition of P did not cause any change of 930 cm^{-1} IR band (i.e. no negative peak at this IR band position). Thus, the IR band representative of symmetric stretching modes of W-O bonds in the WO_4 unit of W (VI) became unaffected in the presence of P. However, the IR band due to W-O antisymmetric stretching vibrations (approx. 830 cm^{-1}) showed a negative intensity in the difference spectrum (Figure 2A1), suggesting a loss of antisymmetric W-O vibration in the presence of P. The symmetrical stretching at 930 cm^{-1} corresponds to only one vibration mode, while the 830 cm^{-1} IR band could be a band coming from the splitting of the degenerated asymmetrical stretching which would be the consequence of an evolution in the speciation. Therefore, the IR data showed evidence that the W (VI)-hematite surface

complexation mode most likely differed in the 'P added later' experimental system compared to the 'W (VI) only' system. However, no release of W (VI) from hematite surface was noticed (Figure 2A1). This could be due to the fact that the surface interactions of W with hematite still occurred as evidenced by the existing W-O symmetric stretching band. Macroscopic sorption envelope data were consistent with the observation that addition of P did not induce any noticeable release of sorbed W (VI) in the pH range studied (pH = 4-11) (Figure 1B).

In situ ATR-FTIR spectra of W (VI) and P competitive sorption, in which P was added first, were presented in Figures 2 B and B1. Final equilibrated P spectrum was shown in Figure 2B and subsequent time series spectra after 100 and 200 µM W (VI) additions were plotted as well. The growth of the W-O stretching band at ~ 932 cm^{-1} increased with time as the IR band (~1092 cm^{-1}) responsible for P surface complexation (Figure 2B) decreased. The difference spectrum clarified this observation (Figure 2B1). Strong W-O stretching band at 932 cm^{-1} in the difference spectrum is suggestive of the surface complexation of W (VI) in the presence of P when P was added first. A weak W-O antisymmetric stretching band can also be found at 831 cm^{-1}. Generally, earlier studies reported similar stronger symmetric stretching IR band in the 929-937 cm^{-1} range in the single ion system at similar pH values for W (VI) sorption on hematite (Rakshit et al., 2017). However, a much stronger antisymmetric stretching band around 831 cm^{-1} was reported in the single ion system compared to the current study with a competitive system (i.e. W (VI) and P), thereby indicating the influence of P on the surface interactions of W (VI) with hematite (Figure 2B1).

Interestingly, W (VI) forced some desorption of P from the hematite surface in the system when P was added first. This is evidenced by a negative peak surrounding the wavenumbers from 1146-969 cm^{-1} in the *in situ* ATR-FTIR spectra (Figure 2 B1). Macroscopic

sorption data of P, in which P was added-first, supported this observation (Figures 1B & Figure S1). In contrast, no negative IR band due to W loss could be identified in the system when P was added later (Figure 2A1). In addition, the formation of the weak antisymmetric W-O stretching band was absent in the difference spectrum of the *in situ* ATR-FTIR experiments, in which P was added later. These contrasting features of the IR data most likely indicate that the W (VI) sorption mechanism differed in the P first and in the P later systems compared to the W (VI) only system.

b) pH Envelope: The *in situ* ATR-FTIR spectra of W (VI) surface complexation on hematite at different pH values were recorded in the presence of P when both W (VI) and P were added simultaneously (Figure 3A & B). Final equilibrated spectra of W (VI) & P were presented at pH range of 4.6-8.05. The initial pH was initiated at 8.05 because the probability of polytungstate surface species formation is higher at acidic pH (< 6) (Hur and Reeder, 2016; Rakshit et al., 2017). Lowering the pH value from 8.05 to 4.6 increased the IR band intensities representing P sorption (~1041-1110 cm^{-1} range for all the pH values, Elzinga and Sparks, 2007) and W (VI) sorption (W-O stretching band ~931-941 cm^{-1} range) on hematite (Figures 3 A & B). The enhancement of IR bands upon lowering pH is indicating increased sorption. The macroscopic data (Figure 1 B) are consistent with this observation. Shifts of both IR bands representing P sorption (~1041-1110 cm^{-1}) and W (VI) sorption (931-941 cm^{-1}) to higher wavenumbers upon decreasing pH value suggest increased degree of inner-sphere sorption, likely due to the evolution of the fraction inner sphere vs the outer sphere bonding, which is consistent with macroscopic pH envelope data (Figure 1A).

In our earlier study, we found strong W-O-W stretching band at 875 cm^{-1} for the pH envelope of W (VI) sorption on hematite in the pH range of 6 to 4.6 (Rakshit et al., 2017). Other

researchers indicated that the presence of this band represents the formation of polytungstate species (Tribalis et al., 2014). Inspection of the IR bands in the present study revealed similar IR bands at 875-877 cm^{-1} in the difference spectra of pH (4.6-8.05, 5.05-8.05, and 6.05-8.05). However, the peak shapes are very different or weaker/broader than the IR bands reported in the study of Rakshit et al. (2017) in the single ion system. Thus, the presence of P has most likely affected the W-O-W stretching frequencies of these surface complexes, thereby indicating that the polytungstate surface species formation may have been somewhat affected.

4. Conclusion

This study reports for the first time detailed surface chemical interactions of tungstate with hematite in a binary mixture with phosphate under environmentally relevant solution properties using *in situ* spectroscopic techniques (e.g. ATR-FTIR). The results indicated that W (VI) sorption on hematite was not affected when W (VI) was added first. However, some influence of P was noticed in the competitive sorption systems, in which either W (VI) & P were added simultaneously or P was added first. Time series spectra of *in situ* ATR-FTIR experiments corroborated these macroscopic observations. In addition, for the binary system, the spectroscopic data suggested that when P was present, the surface complexation mode of W (VI) differed as noted from either the absence of the W-O antisymmetric band or the W-O-W stretching band. Overall, for both W (VI) and P, increasing pH value decreased sorption as evident from both macroscopic and spectroscopic pH envelope data. This study will enhance the

molecular level understanding of W (VI) surface complexation on iron oxides in the presence of competing ions such as P.

Acknowledgements

The author thanks USDA NIFA Evans Allen grant number TENX-1413-CCAP.

References

Charton, P., Gengembre, L., Armand, P., 2002. TeO2-WO3 glasses: Infrared, XPS, and XANES structural characterizations. J. Solid State Chem. 168, 175-183.

Cruywagen, J.J., van der Merwe, I.F.J., 1987. Tungsten (VI) equilibria: A potentiometric and calorimetric investigation. J. Chem. Soc. Dalton Trans. 7, 1701-1705.

Davantés, A., Costa, D., Lefévre, G., 2015. Infrared study of (poly) tungstate ions in solution and sorbed into layered double hydroxides: Vibrational calculations and in situ analysis. J. Phys. Chem. C 119, 12356-12364.

Davantés, A., Lefévre, G., 2015. In situ characterization of (poly) molybdate and (poly) tungstate ions sorbed onto iron (hydr)oxides by ATR-FTIR spectroscopy. Eur. Phys. J. Special Topics 224, 1977-1983.

Davantes, A., Costa, D., Sallman, B., Rakshit, S., and Le'Fevre G. 2017. Surface Polymerization of Mo(VI) and W(VI) Anions on Hematite Revealed by in Situ Infrared Spectroscopy and DFT+U Theoretical Study. Journal of Physical Chemistry C 121 (1), pp 324–332.

Elzinga, E.J., Kretzschmar, R., 2013. *In situ* ATR-FTIR spectroscopic analysis of the co-adsorption of orthophosphate and Cd (II) onto hematite. Geochim. Cosmochim. Ac. 117, 53-64.

Elzinga, E.J., Sparks, D.L., 2007. Phosphate adsorption onto hematite: An in situ ATR-FTIR investigation of the effects of pH and loading level on the mode of phosphate surface complexation. J. Collid Interf. Sci. 308, 53-70.

EPA, 2017. Technical fact sheet-Tungsten. EPA Publication Number: EPA 505-F-17-004.

Fisher, F.J., Pain, D.J., and Thomas, V.G., 2006. A review of lead poisoning from ammunition sources in terrestrial birds. Biol. Conserv. 131, 421-432.

Goldberg, S. 2010. Competitive adsorption of molybdenum in the presence of phosphorus or sulfur on gibbsite. Soil Science, 175, 105-110.

Gustaffson, J.P. 2003. Modelling molybdate and tungstate adsorption to ferrihydrite. Chemical Geology. 200, 105-115.

Hayes, K.E., Papelis, C., Leckie, J.O. 1988. Modeling ionic strength effects on anion adsorption at hydrous oxide/solution interfaces. J. Colloid Interface Sci 125:717-726.

Hur, H., Reeder, R.J., 2016. Tungstate sorption mechanisms on boehmite: Systematic uptake studies and X-ray absorption spectroscopy analysis. J. Colloid Interf. Sci. 461, 249-260.

Iwai, T., Hashimoto, Y., 2017. Adsorption of tungstate (WO_4) on birnessite, ferrihydrite, gibbsite, goethite and montmorillonite as affected by pH and competitive phosphate (PO_4) and molybdate (MoO_4) oxyanions. Applied Clay Science 143, 372-377.

Kashiwabara, T., Takahashi, Y., Marcus, M.A., Urga, T., Tanida, H., Terada, Y., Usui, A., 2013. Tungsten species in natural ferromanganese oxides related to its different behavior from molybdenum in oxic ocean. Geochim. Cosmochim. Ac. 106, 364-378.

Kelly, A.D.R., Lemaire, M., Young, Y.K., Eustache, J.H., Guilbert, C., Molina, M.F., Mann, K.K., 2013. *In vivo* tungsten exposure alters B-cell development and increases DNA damage in murine bone marrow. Toxicological Sciences 131, 434-446.

Koutsospyros, A., Braida, W., Christodoulatos, C., D. Dermatas, Strigul, N., 2006. A review of tungsten: From environmental obscurity to scrutiny. J. Hazard. Mater. 136, 1-19.

Kumar, V.B., Mohanta, D., 2011. Formation of nanoscale tungsten oxide structures and colouration characteristics. Bull. Mater. Sci. 34, 435-442.

Leuz, A-K., H. Mönch, and C.A. Johnson. 2006. Sorption of Sb(III) and Sb(V) to Goethite: Influence on Sb(III) Oxidation and Mobilization. Environ. Sci. Technol. 40: 7277-7282.

Lorenz, E.A., 2009. Role of speciation in tungstate sorption on iron oxyhydroxides: A spectroscopic study. MS thesis, Stony Brook University.

Lorenz, E.A., Hur, H., Reeder, R.J., 2011. Tungstate polymerization and its role in sorption on iron and aluminum oxyhydroxides. Mineral. Mag. 75 (3), 1391.

McBride, M.B., 1997. A critique of diffuse double layer models applied to colloid and surface chemistry. Clays and Clay Minerals 45 no.4, 598-608.

Rakshit, S., Elzinga, E.J., Datta, R., Sarkar, D. 2013a. In situ attenuated total reflectance Fourier-transform infrared study of oxytetracycline sorption on magnetite. J. Environ. Qual. 42:822–827.

Rakshit, S., Dibyendu, S., Elzinga, E.J., Punamiya, P., Datta, R. 2013b. Mechanisms of ciprofloxacin removal by nano-sized magnetite. Journal of Hazardous Materials. 246-247, 221-226.

Rakshit, S., Sallman, B., Davantes, A., and G. Le'Fevre. 2017. Tungstate (VI) Sorption on Hematite: An in situ ATR-FTIR Probe on the Mechanism. Chemosphere 168, pp 685–691.

Seiler, R.L., Stollenwerk, K.C., Garbarino, J.R. 2005. Factors controlling tungsten concentrations in groundwater, Carson Desert, Nevada. Applied Geochemistry. 20, 423-441.

Sheppard, P.R., Ridenour, G, Speakman, R.J., Witten, M.L. 2006. Elevated tungsten and cobalt in airborne particulates in Fallon, Nevada: Possible implications for the childhood leukemia cluster. Applied Geochemistry. 21, 152-165.

Shijun, L., Qiyuan, C., Pingmin, Z., Songqin, L., 1998. Raman spectral study on isopolytungstates in aqueous solution. Trans. Nonferorrous Met. Soc. China. 4, 688-692.

Smith, B.J., Patrick, V.A., 2000. Quantitative determination of sodium metatungstate speciation by 183W N.M.R. spectroscopy. Aus. J. Chem. 53, 965-970.

Steinberg, K.K., Relling, M.V., Gallagher, M.L., Greene, C.N., Rubin, C.S, French, D., Holmes, A.K., Carroll, W.L., Koontz, D.A., Sampson, E.J., Satten, G.A. 2007. Genetic studies of a cluster of acute lymphoblastic leukemia cases in Churchill County, Nevada. Environmental Health Perspectives. 115, 158-164.

Strigul, N., Koutsospyros, A., Arienti, P., Christodoulatos, C., Dermatas, D., Braida, W. 2005. Effects of tungsten in environmental systems. Chemosphere. 61, 248-258.

Sugimoto, T., Sakata, K., Muramatsu, A., 1993. Formation mechanism of monodisperse pseudocubic α-Fe_2O_3 particles from condensed ferric hydroxide gel. J. Colloid Interf. Sci. 159, 372-382.

Sun, J., Bostick, B.C., 2015. Effects of tungstate polymerization on tungsten (VI) adsorption on ferrihydrite. Chem. Geol. 417, 21-31.

Thomas, V.G., Roberts, M.J., and Harrison, P.T.C., 2009. Assessment of the environmental toxicity and carcinogenicity of tungsten-based shot. Ecotoxicology and Environmental Safety 72, 1031-1037.

Tomaszewicz, E., Kaczmarek, S.M., Fuks, H., 2009. New cadmium and rare earth metal tungstates with the scheelite type structure. J. Rare Earth 27, 569-573.

Tribalis, A., Panagiotou, G.D., Tsilomelekis, G., Kalampounias, A.G., Bourikas, K., Kordulis, C., Boghosian, S., Lycourghiotis, A., 2014. J. Phys. Chem. C 118, 11319-11332.

United States Geological Survey. Mineral Commodity Summaries. 2017. Tungsten, 180-181.

Xu, N., Christodoulatos, C., Braida, W. 2006. Adsorption of molybdate and tetrathiomolybdate onto pyrite and goethite: Effect of pH and competitive anions. Chemosphere. 62, 1726-1735.

Xu, N., Christodoulatos, C., Braida, W., 2009. Competitive sorption of tungstate, molybdate, and phosphate mixtures onto goethite. Land Contamination & Reclamation, 17(1), 45-57.

Zorina, M.L., Syristo, L.F., 1972. IR spectra and structures of tungstates. Zhurnal Prikladnoi Spektroskopi 16 (6), 1043-1045.

FIGURE CAPTIONS

Fig. 1

A. W (VI) sorption on 2g L^{-1} hematite as a function of pH(4-10.65) and ionic strength (I=0.01M, 0.1M, and 0.5M NaCl). The initial W conc. = 100µM.

B. The pH envelop for competitive sorption system: W 1st; W, P simultaneous; and P 1st. The pH envelope data from Fig1 A was replotted and marked as W alone for visual comparison with other competitive systems. The concentration of either W (VI) or P was 100µM. The pH range 4 – 10. Ionic strength I = 0.01M NaCl.

Fig. 2

A. The *in situ* ATR-FTIR time series spectra of competitive sorption on hematite where W was added first. Initial W = 100µM. '100 µM W Final' indicates final equilibrated spectra with 100 µM W sorbed on hematite deposit at 0.01 M NaCl. '100 µM P + W Time 1' represents the first IR spectra collected after addition of 100 µM P in the reaction vessel. '100 µM W + P Final' indicates the final equilibrated IR spectra of 100 µM W+P. '200 µM P + 100 µM W' indicates final equilibrated IR spectra after addition of 200 µM P in the reaction vessel.

A1. Difference spectra obtained by subtracting raw spectra of final equilibrated 100µM W from final (200µM P + 100 µM W) raw spectra. I = 0.01M NaCl

B. The *in situ* ATR-FTIR time series spectra of competitive sorption on hematite where P was added first. Initial P = 100µM. '100 µM P Final' indicates final equilibrated spectra with 100 µM P sorbed on hematite deposit in HATR cell at 0.01 M NaCl. '100 µM P + W Time 1' represents the first IR spectra collected after addition of 100 µM W in the reaction vessel. '100 µM P + 200 µM W' indicates final equilibrated IR spectra after addition of 200 µM W in the reaction vessel.

B1. Difference spectra obtained by subtracting raw spectra of final equilibrated 100µM P from final (200 µM W + 100 µM P) raw spectra at I = 0.01M NaCl.

Fig. 3

A. The *in situ* ATR-FTIR spectra of 100µM W + 100µM P sorption (added simultaneously) on hematite at a function of pH values between 4.6 and 8.05 at ionic strength I=0.01M NaCl.

A1. Resultant difference spectra derived from subtracting each subsequent lower pH spectra from pH 8.05 spectra.

Fig. 1

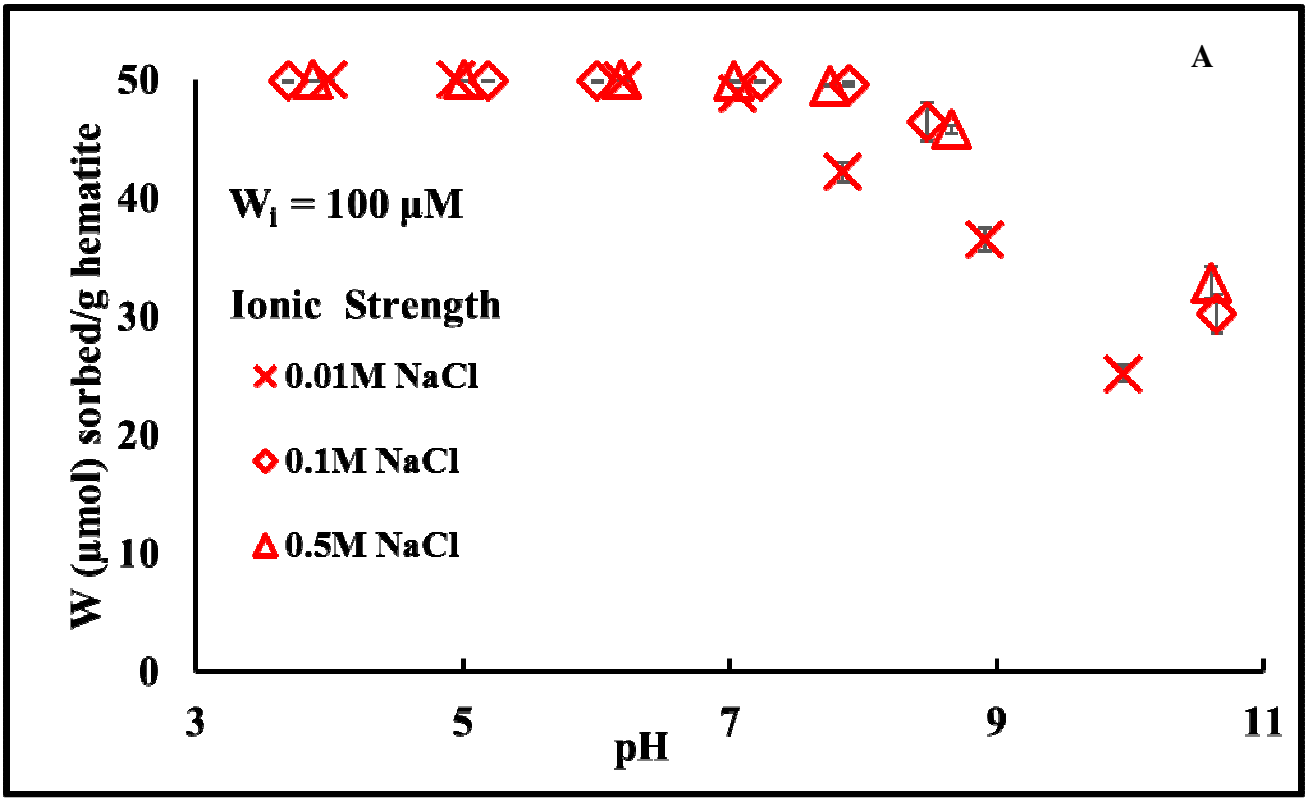
A
W (µmol) sorbed/g hematite
50
40
30
20
10
0
3
5
7
9
11
pH
W$_i$ = 100 µM
Ionic Strength
0.01M NaCl
0.1M NaCl
0.5M NaCl

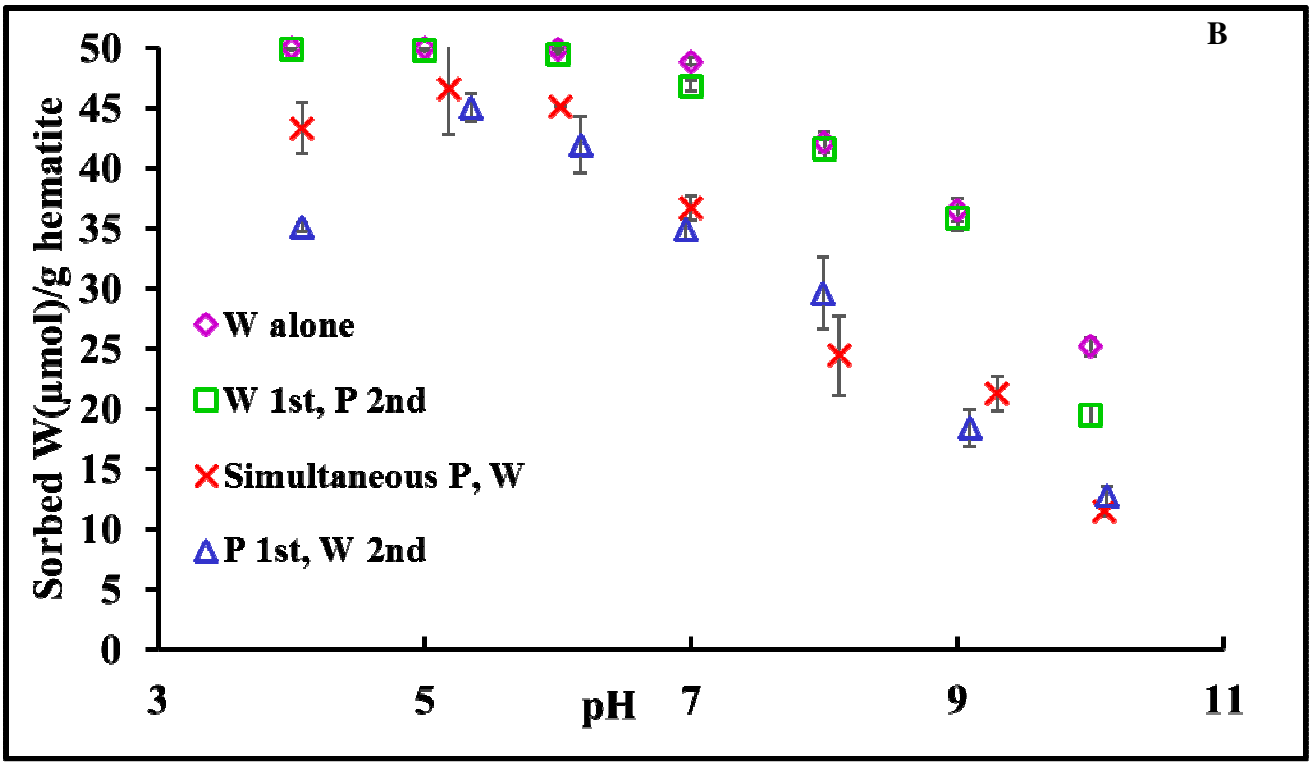
B
Sorbed W(µmol)/g hematite
50
45
40
35
30
25
20
15
10
5
0
3
5
pH
7
9
11
W alone
W 1st, P 2nd
Simultaneous P, W
P 1st, W 2nd

Fig. 2

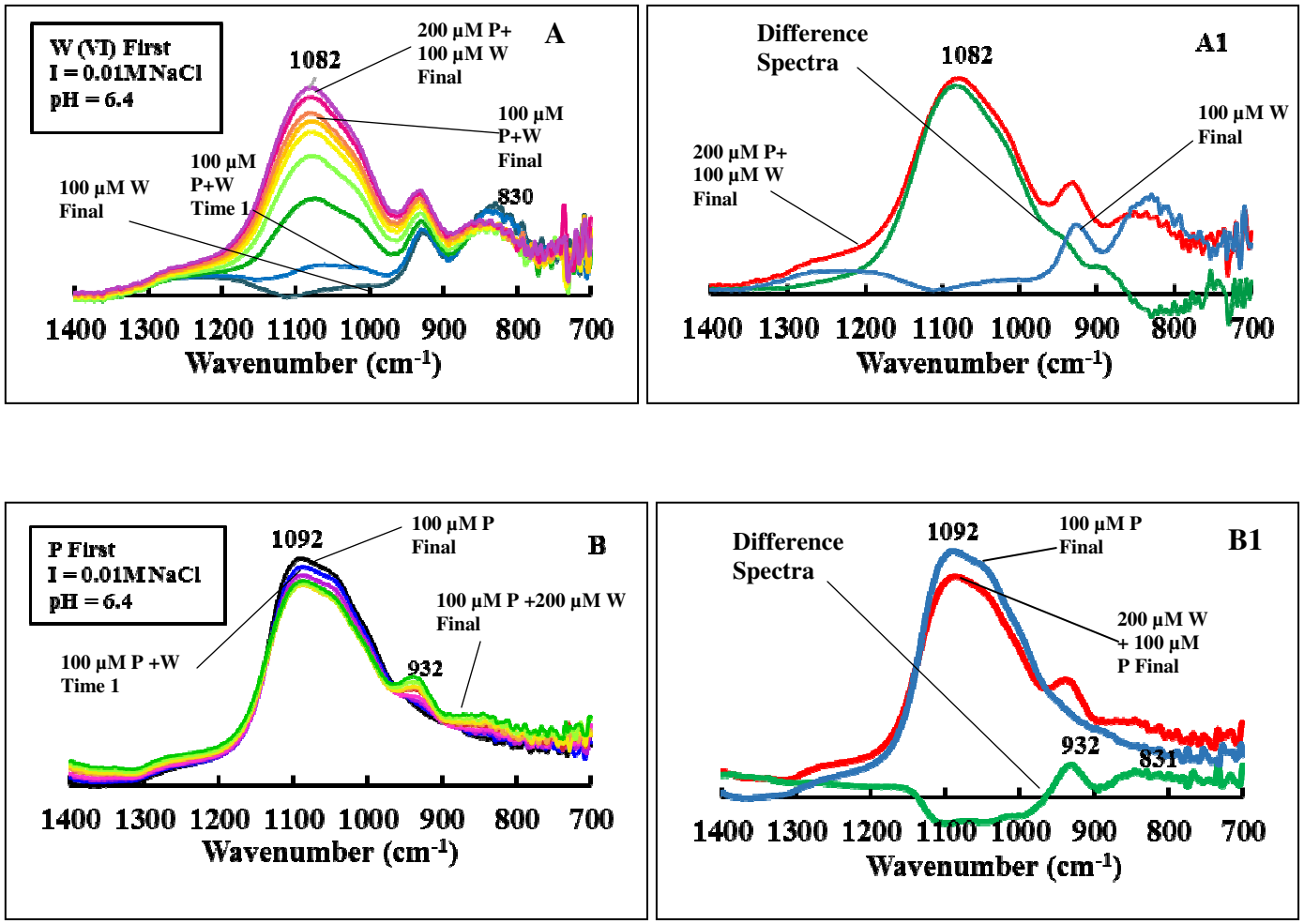
W (VI) First
I = 0.01M NaCl
pH = 6.4
A
1082
200 µM P+
100 µM W
Final
100 µM
P+W
Final
100 µM
P+W
Time 1
100 µM W
Final
830
1400 1300 1200 1100 1000 900 800 700
Wavenumber (cm-1)
Difference
Spectra
A1
1082
100 µM W
Final
200 µM P+
100 µM W
Final
1400 1300 1200 1100 1000 900 800 700
Wavenumber (cm-1)
P First
I = 0.01M NaCl
pH = 6.4
B
1092
100 µM P
Final
100 µM P +200 µM W
Final
100 µM P +W
Time 1
932
1400 1300 1200 1100 1000 900 800 700
Wavenumber (cm-1)
Difference
Spectra
B1
1092
100 µM P
Final
200 µM W
+ 100 µM
P Final
932
831
1400 1300 1200 1100 1000 900 800 700
Wavenumber (cm-1)

Fig. 3

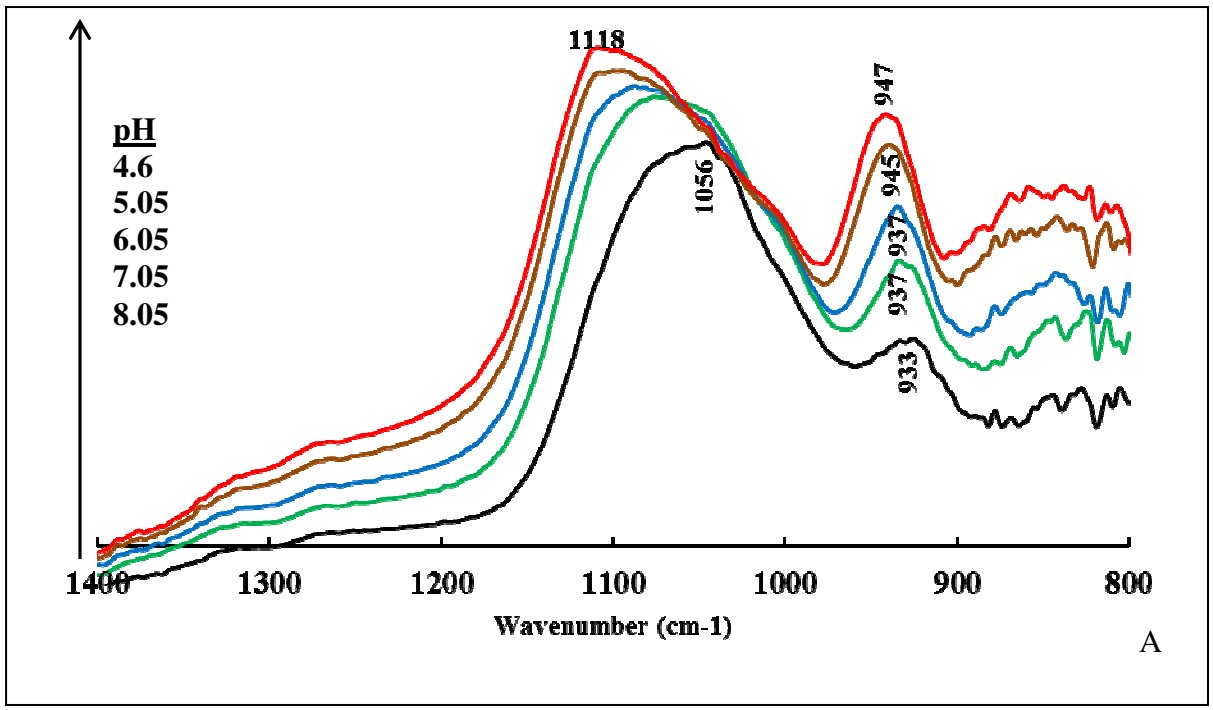
pH
4.6
5.05
6.05
7.05
8.05
1118
1056
947
945
937
937
933
1400
1300
1200
1100
1000
900
800
Wavenumber (cm-1)
A

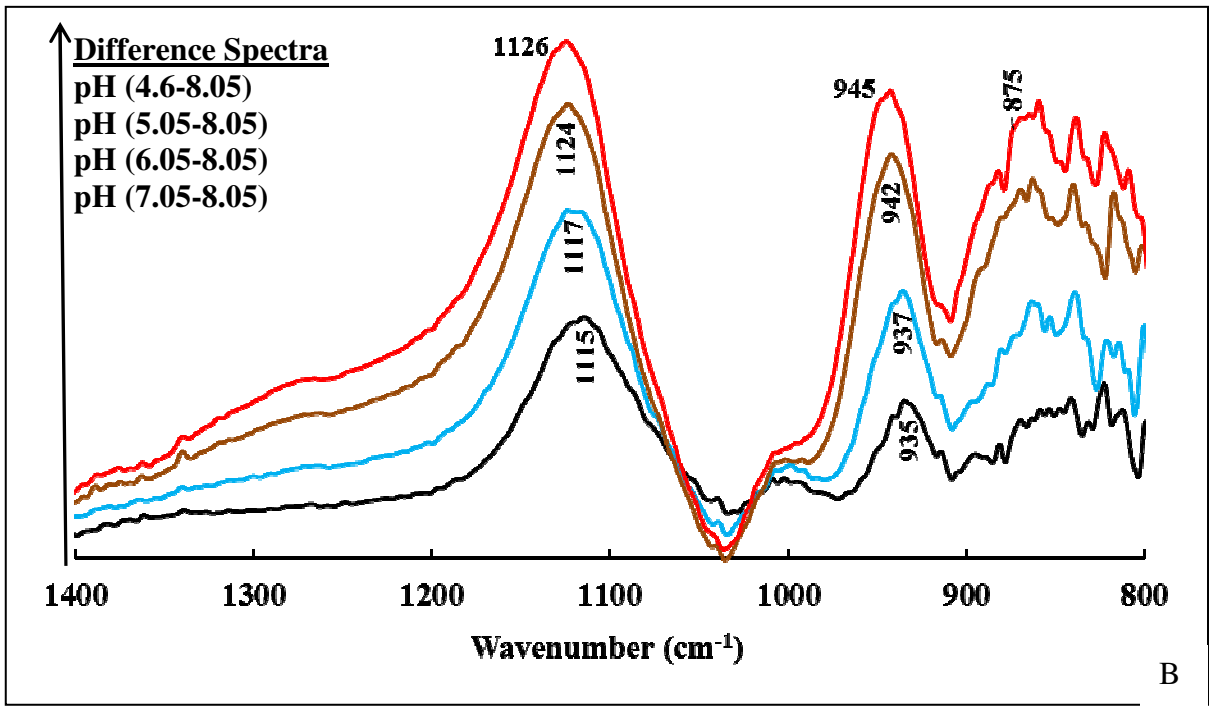
Difference Spectra
pH (4.6-8.05)
pH (5.05-8.05)
pH (6.05-8.05)
pH (7.05-8.05)
1126
1124
1117
1115
945
942
937
935
875
1400
1300
1200
1100
1000
900
800
Wavenumber (cm-1)
B